NIH Public Access
Author Manuscript
Apoptosis. Author manuscript; available in PMC 2015 April 01.

Published in final edited form as:
Apoptosis. 2014 April ; 19(4): 748–758. doi:10.1007/s10495-013-0960-1.

Induction of autophagy-dependent cell death by the survivin suppressant YM155 in salivary adenoid cystic carcinoma

Yu-Fan Wang,
The State Key Laboratory Breeding Base of Basic Science of Stomatology & Key Laboratory of Oral Biomedicine Ministry of Education, Department of Oral and Maxillofacial-Head and Neck Oncology, School and Hospital of Stomatology, Wuhan University, Wuhan 430079, China

Wei Zhang,
The State Key Laboratory Breeding Base of Basic Science of Stomatology & Key Laboratory of Oral Biomedicine Ministry of Education, Department of Oral and Maxillofacial-Head and Neck Oncology, School and Hospital of Stomatology, Wuhan University, Wuhan 430079, China

Ke-Fei He,
The State Key Laboratory Breeding Base of Basic Science of Stomatology & Key Laboratory of Oral Biomedicine Ministry of Education, Department of Oral and Maxillofacial-Head and Neck Oncology, School and Hospital of Stomatology, Wuhan University, Wuhan 430079, China

Bing Liu,
The State Key Laboratory Breeding Base of Basic Science of Stomatology & Key Laboratory of Oral Biomedicine Ministry of Education, Department of Oral and Maxillofacial-Head and Neck Oncology, School and Hospital of Stomatology, Wuhan University, Wuhan 430079, China

Lu Zhang,
The State Key Laboratory Breeding Base of Basic Science of Stomatology & Key Laboratory of Oral Biomedicine Ministry of Education, Department of Oral and Maxillofacial-Head, and Neck Oncology, School and Hospital of Stomatology, Wuhan University, Wuhan 430079, China

Wen-Feng Zhang,
The State Key Laboratory Breeding Base of Basic Science of Stomatology & Key Laboratory of Oral Biomedicine Ministry of Education, Department of Oral and Maxillofacial-Head and Neck Oncology, School and Hospital of Stomatology, Wuhan University, Wuhan 430079, China

Ashok B. Kulkarni,
Functional Genomics Section, Laboratory of Cell and, Developmental Biology, National Institute of Dental and Craniofacial Research, National Institutes of Health, Bethesda, MD 20892, USA

Yi-Fang Zhao, and

© Springer Science+Business Media New York 2013

Correspondence to: Yi-Fang Zhao; Zhi-Jun Sun, zhijundejia@163.com.

Y.-F. Wang and W. Zhang contributed equally to this study.

Electronic supplementary material The online version of this article (doi:10.1007/s10495-013-0960-1) contains supplementary material, which is available to authorized users.

Conflict of interest No potential conflict of interest was disclosed.

NIH-PA Author Manuscript
NIH-PA Author Manuscript
NIH-PA Author Manuscript

NIH-PA Author Manuscript

NIH-PA Author Manuscript

NIH-PA Author Manuscript

The State Key Laboratory Breeding Base of Basic Science of Stomatology & Key Laboratory of Oral Biomedicine Ministry of Education, Department of Oral and Maxillofacial-Head and Neck Oncology, School and Hospital of Stomatology, Wuhan University, Wuhan 430079, China

Zhi-Jun Sun

The State Key Laboratory Breeding Base of Basic Science of Stomatology & Key Laboratory of Oral Biomedicine Ministry of Education, Department of Oral and Maxillofacial-Head and Neck Oncology, School and Hospital of Stomatology, Wuhan University, Wuhan 430079, China

Yu-Fan Wang: yifang@whu.edu.cn; Zhi-Jun Sun: zhijundejia@163.com

Abstract

Adenoid cystic carcinoma (ACC) is one of the most common malignancies of the major and minor salivary glands. However, the molecular mechanism underlying the aggressive growth of human salivary ACC remains unclear. In the present study, we showed that survivin, which belongs to the family of inhibitors of apoptosis, is closely related to the high expression of CDK4 and cyclin D1 in human ACC specimens. By employing the smallmolecule drug YM155, we found that the inhibition of survivin in ACC cells caused significant cell death and induced autophagy. Chloroquine, an autophagy inhibitor, prevented cell death induced by YM155, suggesting YM155-induced autophagy contributed to the cell death effects in ACC cells. More importantly, evidence obtained from a xenograft model using ACC-2 cells proved the occurrence of YM155-induced autophagy and cell death in vivo was correlated with the suppression of Erk1/2 and S6 activation as well as increased TFEB nuclear translocation. Taken together, our results indicate YM155 is a novel inducer of autophagy-dependent cell death and possesses therapeutic potential in ACC.

Keywords

Survivin; Adenoid cystic carcinoma; YM155; Apoptosis; Autophagy

Introduction

Adenoid cystic carcinoma (ACC) is a malignant epithelial glandular type neoplasia, characterized by neural infiltration, rich in angiogenesis, high incidence of distant metastasis and poor long-term survival rates [1]. To date, no systematic and effective strategy for improving the treatment of ACC is available. Surgery followed by postoperative radiotherapy and/or chemotherapy is considered as the preferred therapy for ACC, however, both are ineffective for its local recurrence and distant metastasis [2]. Understanding the molecular mechanism underlying the aggressive growth of ACC will benefit the personalized and molecular target therapy [3].

Apoptosis resistance is a hallmark for most cancers, by which malignant cells escape from cell death [4]. Among the process, inhibitors of apoptosis (IAPs) family members play an important role, and more importantly, they are highly proved high expressed in many cancers [5, 6]. Survivin, the most important member of IAP family, is reported to be highly expressed in ACC and it is commonly associated with poor prognosis and survival of the

NIH-PA Author Manuscript

NIH-PA Author Manuscript

NIH-PA Author Manuscript

patient [7]. Survivin has been implicated in both cell survival and cell cycle regulation in many types of cancers by acting with p53 and/or CDK complex. YM155, a novel smallmolecule drug that inhibits survivin at the mRNA level [8], is currently being used in phase I and phase II clinical studies in advanced solid tumors [9, 10]. Thus, it may be a promising choice for ACC therapy by targeting survivin via administration of YM155. However, the underlying mechanism by which YM155 induces cancer cell death remains unclear, especially in ACC cells. Recent research has proven that suppression of survivin by YM155 can induce autophagy-dependent apoptosis in prostate cancer [11], indicating autopohagy may be a novel mechanism of ACC in response to YM155.

Autophagy in cancer is believed to be involved in both survival pathways and cell death [12-14]. Autophagy is a conservative process of protein degradation through autophagosome and lysosome system [15]. Autophagy regulation involves multiple autophagy-specific genes (ATGs), and in which mTOR complex1 (mTORC1) and Beclin1 (ATG6) complex are extremely important for autophagosome induction and elongation [16, 17]. Recent research has also suggested that transcription factor EB (TFEB), which belongs to the MiT family, plays an important role in tumourigenesis [18], autophagosome [15] and lysosome biogenesis [19]. Moreover, limited data suggest that mTORC1 [20] and phosphorylation of Erk [21] are two important signaling pathways that regulate the nuclear localization of TFEB by promoting phosphorylation in the serine-rich motif. mTOR is a potent inhibitor of TFEB nuclear translocation and TFEB is a rapamycin-resistant substrate of mTORC1 [6]. In normal status, mTOR phosphorylated TFEB on serine 211 which results the inhibition of TFEB activity. When mTOR is inactive, dephosphorylation of TFEB was detected, which leads TFEB accumulation in the nucleus [22]. What's more interesting, some researches also detected coimmunoprecipitation of Erk2–TFEB in normal but not in starved medium. And knockdown of Erk1/2 proteins by small interfering RNA could induce TFEB nuclear translocation to a similar extent as serum starvation [23]. Thus, we believe that the mechanism of action of YM155 in ACC is correlated with these pathways.

In this study, we aimed to answer whether the inhibition of survivin by YM155 can induce ACC cell death and autophagy, and to explain this phenomenon by exploring the molecular mechanism of YM155 in inhibiting ACC.

Materials and methods

Patients and immunohistochemistry

Thirty pathologically confirmed human ACC specimens, with ten normal salivary gland tissues were collected at the Hospital of Stomatology, Wuhan University. The procedures were performed in accordance with the guidelines of National Institutes of Health regarding the use of human tissues and approved by the institute review board of the Ethics Committee of the Hospital of Stomatology, Wuhan University. Immunohistochemistry was performed as previous described [24] by incubating with survivin (1:200; Cell Singling Technology, MA, USA), CDK4 (1:200; Abcam, MA, USA), CyclinD1 (1:500; Santa Cruz, CA, USA) or p-Rb^{S780} (1:200; Abcam, MA, USA) antibody overnight at 4 °C. The antibody binding was detected by horseradish peroxidase-conjugated secondary antibody using a diaminobenzidine substrate kit (Dako, CA, USA) according to the manufacturer's protocol

NIH-PA Author Manuscript

NIH-PA Author Manuscript

NIH-PA Author Manuscript

as previous described [24]. The negative control slides were obtained by using PBS buffer instead of the primary antibody. For analysis, as we previous reported [23], slices were scanned with background substrate for each slice using an Aperio ScanScope CS scanner, and quantified using Aperio Quantification software (Version 9.1) for membrane, nuclear, or pixel quantification. Histoscore of the staining for membrane or nuclear was calculated as the percentage of positive cells by the formula: (3+) × 3 + (2+) × 2 + (1+) × 1. And the histoscore of pixel quantification was calculated as total intensity/total cell number.

Cell culture, drugs, and reagents

Human adenoid cystic carcinoma (ACC-2 and ACC-M) cell lines were cultured in DMEM containing 10 % fetal bovine serum as previous described [25]. YM155 (Selleck, TX, USA) was dissolved in DMEM to produce a stock solution that was aliquot and stored at −20 °C. Chloroquine (CQ, Sigma, MO, USA) was dissolved in DMEM to produce a 10 μmol/L stock solution that was aliquoted and frozen at −20 °C. 3-Methyladenine (3-MA, Sigma) was also dissolved in DMEM to produce a 4 mmol/L stock solution and frozen at −20 °C.

Nude mice xenografts

Female BALB/c nude mice (18–20 g) with 6–8 weeks of age were housing in the Experimental Animal Center of Wuhan University in pressurized ventilated cages according to institutional regulations. All proposals were approved and supervised by the institutional animal care and use committee of Wuhan University. ACC-2 cells (2×10^6 in 0.2 mL of medium) were inoculated subcutaneously into the flank of the mice. After 7 days, tumor-bearing mice were randomly divided into three groups, which were intraperitoneal injection PBS (Vehicle group, $n = 5$), YM155 5 mg/kg ($n = 5$) for 14 consecutive days or YM155 10 mg/kg ($n = 4$) for 3-day continuous infusion per week for 2 weeks. Tumor volumes were calculated to determine the tumor growth according to the formula ($\text{width}^2 \times \text{length}$)/2 as previous described [26]. The mice were weighted every other day to evaluate the toxicity of the drug. The mice were euthanized at day 30, and the tumors were harvested, photographed, and then embedded in paraffin for immunohistochemical analysis or frozen at −80 °C for western blotting [26].

Cell proliferation assay

Cell proliferation was accessed by 3-(4,5-dimethylthiazol- 2-yl)-2,5-diphenyltetrazoliumbromide (MTT) assay as previously described [27]. Briefly, ACC-2 cell lines were treated with the indicated concentrations of YM155 in DMEM for 24 h. Media was removed and cells were resuspended with DMEM and 10 % MTT. After 4 h incubation, the media was removed and DMSO was added to dissolve purple crystallization. Then read absorbance at 570 nm with a reference filter of 620 nm.

Cell death detection ELISA

ACC-2 cell line was incubated in a 96-well plate with the indicated concentrations of YM155 for 24 h [26]. After the incubation, the cells were pelleted by centrifugation and the supernatant was discarded. Cells were resuspended and incubated in lysis buffer. After centrifugation, an aliquot of the supernatant was transferred to a streptavidin-coated well of

NIH-PA Author Manuscript

NIH-PA Author Manuscript

NIH-PA Author Manuscript

a microtiter plate. Nucleosomes were bound in the supernatant with anti-histone and anti-DNA. Then the immobilized antibody–histone complexes were washed three times and sample was incubated with peroxidase substrate. At last, the amount of colored product was determined using spectrophotometer.

Annexin V/PI staining

After YM155 treatment as previously described (0, 5, 10 and 20 nM), ACC cells were detached from culture dishes by trypsin–EDTA and centrifuging. Annexin V/PI (BD Pharmingen) staining were performed according to manufacture's instruction and cell counted by flow cytometer (BD) as previous described [26].

Hoechst and MDC staining

Treated ACC-2 cells were treated as described previously [25]. Treated cells were stained with Hoechst 33258 (5 μg/mL) or monodansylcadaverine(MDC, 50 mmol/L) mixture solution at room temperature for 30 min. The staining was visualized and captured under an inverted fluorescent microscope (Leica).

LC3 immunofluorescence staining

ACC cells were seeded to a coverglass slide chamber (Millipore), and after the designated treatments, cells were washed with PBS three times. Then fixed with 4 % paraformaldehyde in PBS for 15 min at room temperature, and permeabilized with 0.3 % Triton X-100 for 10 min. Cells were washed with PBS and blocked with 2.5 % BSA in PBS for 1 h. Then incubated with LC3 primary antibody (1:200; Cell Signaling Technology, MA, USA) overnight at 4 °C, followed by second antibody. The coverglass was examined and recorded by a fluorescent microscope and representative cells were selected and photographed [25]. Cells with more than 5 bright LC3 dot punctae in the cytoplasm surrounding the nuclear were consider as a LC3-positive cells. LC3 dot punctae were quantified according to the guideline in detect autophagy by counting percentage of LC3-positive cell [6].

Western blotting

ACC cell lines were treated with the indicated concentrations of YM155 pretreated with or without CQ for 24 h. Then the cells were lysed, and the total protein was separated using 12 % SDS-polyacrylamide gel electrophoresis and transferred onto polyvinylidene fluoride membranes (Millipore Corporation, MA, USA). The blots were then blocked with 5 % non-fat dry milk at room temperature for 1 h, and incubated overnight at 4 °C with the corresponding primary antibodies at dilutions recommended by the suppliers, followed by incubation with horseradish peroxidase-conjugated secondary antibody (Santa Cruz) for 0.5 h. Then blots were developed by West Pico enhanced chemiluminescence detection kit (Thermo). GAPDH was detected on the same membrane and used as a loading control [27].

Hierarchical clustering and statistical analysis

The staining scores that resulted from immunohistochemical analyses of human tumor samples were converted into scaled values centered on zero in Microsoft Excel. The hierarchical analysis was done using Cluster 3.0 with average linkage based on Pearson's

NIH-PA Author Manuscript

NIH-PA Author Manuscript

NIH-PA Author Manuscript

correlation coefficient as the selection variable on the unsupervised approach. The results were visualized using Java TreeView 1.0.5 as described previously [24]. The clustered data were arranged with markers on the horizontal axis and tissue samples on the vertical axis. Two biomarkers with a close relationship are located next to each other.

Data analyses were conducted using Graph Pad Prism version 5.00 for Windows (Graph-Pad Software Inc.). One-way ANOVA followed by the post-Dunnett or Bonferroni multiple comparison tests were used to analyze the differences in protein levels as compared with control group or among each group. The Mann–Whitney *U* test and Student *t* test was used to evaluate differences in the proteins immunohistochemistry and total tumor area of the mice YM155-treated and vehicle only group. Log rank statistics were used to evaluate survival in the YM155 and control groups. Mean values ± SEM with a difference of $P < 0.05$ were considered as statistically significant.

Results

High expression of survivin/CDK4/CyclinD1/p-Rb in human salivary gland ACC

The basal expression levels and activation status of survivin, CDK4, cyclin D1 and p-Rb^{S780}, which are the key proteins in cell cycle regulation, were determined. Our results revealed that survivin, CDK4, cyclin D1 and p-Rb^{S780} were highly expressed in all three pathological types of ACC compared with pericancerous normal salivary gland tissues (Fig. 1a, b). Expression of survivin was positively correlated with the high expression of CDK4 ($P < 0.0001$, $r = 0.7198$), cyclin D1 ($P = 0.0029$, $r = 0.4490$) and p-Rb^{S780} ($P = 0.0157$, $r = 0.3707$). The sample included ACC tissue ($n = 30$) and normal salivary gland tissue ($n = 10$, Fig. 1b, Supplementary Fig. 1).

YM155-induced cell death in ACC-2 cell line

We examined whether or not YM155, a novel inhibitor of survivin, can induce ACC cell death. MTT assay showed that YM155 could inhibit the growth of ACC-2 (Fig. 2a, IC50 = 10 nmol/L) and ACC-M cell lines (Supplementary Fig. 2a, IC50 = 20 nmol/L) in a dose-dependent manner. In Fig. 2c, chromatin condensation was observed by Hoechst 33258 staining assay in ACC-2 treated with YM155. Moreover, by assessing the DNA fragmentation in YM155- treated ACC cells using the Cell Death Detection $ELISA^{PLUS}$ kit (Fig. 2b) and Annexin V (+) and PI (∓) % cells using flow cytometry (Fig. 2d), we proved that YM155 caused the cell death in an apoptosis dependent manner. As detected in Annexin V (−) and PI (+) % cells, we find YM155 induces ACC-2 death by not only apoptosisdependent pathway but also non-apoptotic pathway. In addition, we showed the increase in cleaved PARP was related to low expression of survivin by YM155 inhibition in ACC-2 (Fig. 2e with quantification in Fig. 2f). In addition, YM155 induces ACC-2 cell death by not only apoptosis-dependent pathway but also by non-apoptotic pathway since significant Annexin V(−) PI(+) % increase especially treated with 20 nM YM155 for 24 h. These data suggest that YM155 can inhibit the growth of ACC by inducing cell death.

NIH-PA Author Manuscript

NIH-PA Author Manuscript

NIH-PA Author Manuscript

YM155 induced autophagy in ACC-2 cell line

Since autophagy is closely related to apoptosis and survivin plays an important role in both apoptosis and autophagy, the role of survivin in autophagy is interesting to explore. We found that autophagy was increased after YM155 treatment by MDC (Fig. 3a). And exposure to YM155 led to an obvious punctuate pattern of LC3II immunofluorescence staining in ACC-2 (Fig. 3b). Based on these observations, we further used chloroquine (CQ), a reagent confirmed to block the fusion between autophagosomes and lysosomes, to determine whether or not LC3 conversion induced by YM155 proceeds to the last step of lysosomal degradation. The results suggest that 10 and 20 nM YM155 can significantly increase the conversion of LC3I to LC3II, which indicates the presence of more mature autophagosomes (Fig. 3c with quantification in Fig. 3d). Artificial inhibition of the fusion of autophagosomes and lysosomes by CQ was proven to accumulate YM155- induced LC3II in ACC cell lines (Fig. 3c, d).

YM155-induced autophagy enhances cell death in ACC

Based on the above observations, we determined whether the autophagy induced by YM155 serves as a prosurvival or prodeath mechanism. Figure 3c, d show that cleaved PARP decreases in cells treated with CQ. We then used a putative autophagy inhibitor, 3-MA, which prevents the induction of autophagosomes to inhibit autophagy flux, and tested its effect on YM155-induced cell death. Cells treated with 3-MA reduced YM155-induced cell death in ACC-2 cell lines, as determined by flow cytometry (Fig. 3e). These results collectively demonstrate that autophagy induced by YM155 contributes to the induced cell death in ACC cell lines.

YM155 inhibited tumourigenesis of ACC-2 xenografts

To further authenticate the growth inhibition ability of YM155 in vivo, ACC-2 xenografts in nude mice were established. Figure 4a shows the different drug delivery strategies. The growth of ACC-2 xenograft tumors was significantly inhibited by YM155 treatment in a dosedependent manner relative to the vehicle only group (Fig. 4b–e); toxicity to the mice towards high doses of YM155 was also observed (Fig. 4f). As such, we examined only the low-dose YM155 and vehicle groups for subsequent Western blot and immunohistochemistry.

YM155-induced cell death and autophagy by inhibiting the phosphorylation of Erk and mTOR pathway

We found that the expression of survivin decreased in the ACC-2 xenografts treated with YM155 (Fig. 5a, b). We observed increase in TUNEL+ cells (Fig. 5a) as well as increase in cleaved PARP and caspase 3 in theYM155-treated group compared with the vehicle-only group (Fig. 5b), as determined by Western blot. These findings indicate that the decrease in tumourigenesis is caused by an increase in apoptosis. YM155 was found to induce autophagy by observations of increases in LC3II and SQSTM1, two markers of autophagy, in ACC xenografts by Western blot as well as increases in Beclin1 in immunostaining (Fig. 5a, b). To further investigate the mechanism of YM155 in ACC, we focused on TFEB, a master molecule that regulates autophagy. Our data suggested that nuclear translocation of

NIH-PA Author Manuscript

NIH-PA Author Manuscript

NIH-PA Author Manuscript

TFEB afterYM155 treatment inACC xenograft increases compared with the vehicle-only group, as determined by immunohistochemistry (Fig. 6a). Phosphorylation of the two important signaling pathways of Erk and S6 also decreased (Fig. 6a, b). All of the results presented above are consistent with our in vitro findings, which demonstrate that YM155 increases autophagy by inhibiting phosphorylation of Erk and mTOR, and by increasing the nuclear translocation of TFEB.

Discussion

YM155, a novel imidazolium-based compound, selectively suppresses survivin expression in most cells [8]. YM155 has been proven to induce apoptosis in prostate cancer as well as other cancers [11] and shown to have antitumor effects in various tumor xenograft models [28]. In combination with YM155, transitional anti-carcinogenic drugs, such as platinum compounds or docetaxel, show enhanced anticancer efficacy in various cancer cells in vitro and in vivo. Phase I and II clinical trials on YM155 have been performed and conducted to be safe during the therapeutics, showing the promising application of the compound in cancer clinical treatment. However, the effects ofYM155 on human ACC, a specific carcinoma characterized by diffused invasion of the tumor into adjacent organs and early distant metastasis remains unknown. In the current study, we have demonstrated that YM155 could halt ACC progression by inducing cell death and autophagy in vitro as well as in vivo.

Recent evidence indicates that apoptosis and autophagy occur almost simultaneously during treatment with anti-cancer drugs [29] since they share many of the same cellular regulators [30]. However, whether or not autophagy exerts pro-death or pro-survival effects on cancer cell death remains ambiguous and must be addressed. Accumulating evidence suggests has shown that autophagy is used as a prosurvival mechanism in some cancer cells and attenuates anticancer drug-induced apoptosis [31]. On the other hand, autophagic cell death has shown as an important cell death mechanism in response to certain anti-cancer drugs [32]. In the present study, we found thatYM155 can induce both cell death and autophagy in ACC-2 cells as wells as in xenografts established by implanting ACC-2 cells in nude mice. To delineate the role of autophagy induced by YM155 in ACC, 3-MA, an inhibitor of autophagy, was used. Results showed that suppression of autophagic flux significantly decreases the cell death induced by YM155 in both cell lines and xenografts, which suggests that an increase in autophagic flux may act as a cell death mechanism in ACC cells.

To further explore the mechanism of YM155-induced cell death and autophagy, as well as the role of survivin in each process, possible proteins involved were detected in xenografts by Western blot. The expression of Beclin1 was up-regulated in tumors treated with YM155. Bcl-2, which has been proven to be highly expressed in ACC tissues by high throughput scanning and validation [1, 33], could inhibit Beclin1-dependent autophagic activation by directly binding Beclin1 protein [16]. Previous data also suggest that survivin exhibits novel interaction with Beclin1, which plays an important role in autophagy [34]. Some researchers have shown that survivin can inhibit the evolution of the LC3 punctate pattern in prostate cancer and the same was observed in ACC cell lines and nude mice [35]. In spite of using bioinformatics analysis- based and prediction, we did not observe the direct binding of

NIH-PA Author Manuscript

NIH-PA Author Manuscript

NIH-PA Author Manuscript

survivin with other ATG proteins. We propose that the mechanism of YM155-induced autophagy may be attributable to the down-regulation survivin as well as Bcl-2, thereby releasing LC3 to activate autophagy. These findings indicate that survivin is a key molecule in the interaction between autophagy and apoptosis.

Decreases in phosphorylation of Erk and S6 by YM155 treatment were observed, consistent with the results of other researches demonstrating YM155 inhibit survivin via the Erk pathway in pancreatic cancer [36]. We believe that the down-regulation of survivin induced by YM155 in ACC may be partly due to inhibition of Erk pathway. Interestingly, the downstream molecule of mTORC1, which plays an important role in protein biosynthesis [37], ribosomal protein S6 kinase 1 (S6K1) was also down-regulated at the phosphorylation level. Therefore, it is valid to say that mTOR/S6 may act downstream of Erk as reported in previous studies [36]. Interestingly, TFEB, which has been demonstrated to play as a downstream protein of mTOR in other cancer cells, was found to increase in tumors treated with YM155, as determined by immunohistochemical analyses. TFEB that regulated lysosome trafficking, which is an important process during autophagolysosome formation, can lead to the dephosphorylation and translocation into the nucleus by mTOR [38, 39]. Recent reports also prove that knockdown of Erk proteins can also induce TFEB nuclear translocation [19]. Taken together, our data suggest that YM155-regulated TFEB activation which might be dependent on the Erk and/or S6 pathway involved in its induced autophagy, at least in ACC cells.

Since YM155 may be a potential drug target for ACC chemotherapy, understanding its toxicity in mice is important. This conducted the administration methods or drug delivery system application. Previous studies have proven that controlled release using osmotic pump or nanoparticles at the sub-nanomolar range in pre-clinical models show less toxicity than other delivery method [8]. In the present study, we found that the weight of mice largely decreased when the drug delivery strategy is 10 mg/kg, and the tumor growth was also significantly inhibited. This finding indicates that systemic toxicity of YM155 may be observed when the applied dose is greater than or equal to 10 mg/kg, and which means the better drug delivery strategy of YM155 is 5 mg/kg or less in 2 weeks. Our data suggest that continual low-dose infusion may be a good delivery method for at least ACC xenograft. Controlled-release methods may be a promising strategy for YM155-based chemotherapy.

In summary, the current study demonstrated that YM155, a novel inhibitor of survivin, can suppress tumourigenesis of ACC in vitro and in vivo by inducing cell death and autophagy in an Erk-and mTOR-dependent manner. YM155-induced autophagy might contribute to the anti-tumour effects. Our study provided a novel strategy for ACC chemotherapy using YM155, a survivin suppressant, and partially uncovered the underlying mechanism involved in the functions of the compound.

Supplementary Material

Refer to Web version on PubMed Central for supplementary material.

NIH-PA Author Manuscript

NIH-PA Author Manuscript

NIH-PA Author Manuscript

Acknowledgments

This work was supported by grants from National Natural Science Foundation of China (81072203, 81272963) to Z.-J. Sun (81371106) to L. Zhang (81272946) to W.-F. Zhang and (81170977) to Y.-F. Zhao. Fundamental Research Funds for the Central Universities of China (2012304020203) to W. Zhang.

References

1. Vekony H, Ylstra B, Wilting SM, et al. DNA copy number gains at loci of growth factors and their receptors in salivary gland adenoid cystic carcinoma. Clin Cancer Res. 2007; 13:3133–3139. [PubMed: 17545515]
2. Laurie SA, Ho AL, Fury MG, Sherman E, Pfister DG. Systemic therapy in the management of metastatic or locally recurrent adenoid cystic carcinoma of the salivary glands: a systematic review. Lancet Oncol. 2011; 12:815–824. [PubMed: 21147032]
3. Ramalingam SS, Kummar S, Sarantopoulos J, et al. Phase I study of vorinostat in patients with advanced solid tumors and hepatic dysfunction: a National Cancer Institute Organ Dysfunction Working Group study. J Clin Oncol. 2010; 28:4507–4512. [PubMed: 20837947]
4. Brown JM, Attardi LD. The role of apoptosis in cancer development and treatment response. Nat Rev Cancer. 2005; 5:231–237. [PubMed: 15738985]
5. Schimmer AD. Inhibitor of apoptosis proteins: translating basic knowledge into clinical practice. Cancer Res. 2004; 64:7183–7190. [PubMed: 15492230]
6. Khan S, Jutzy JM, Aspe JR, McGregor DW, Neidigh JW, Wall NR. Survivin is released from cancer cells via exosomes. Apoptosis. 2011; 16:1–12. [PubMed: 20717727]
7. Schlette EJ, Medeiros LJ, Goy A, Lai R, Rassidakis GZ. Survivin expression predicts poorer prognosis in anaplastic large-cell lymphoma. J Clin Oncol. 2004; 22:1682–1688. [PubMed: 15117990]
8. Nakahara T, Kita A, Yamanaka K, et al. YM155, a novel small-molecule survivin suppressant, induces regression of established human hormone-refractory prostate tumor xenografts. Cancer Res. 2007; 67:8014–8021. [PubMed: 17804712]
9. Satoh T, Okamoto I, Miyazaki M, et al. Phase I study of YM155, a novel survivin suppressant, in patients with advanced solid tumors. Clin Cancer Res. 2009; 15:3872–3880. [PubMed: 19470738]
10. Giaccone G, Zatloukal P, Roubec J, et al. Multicenter phase II trial of YM155, a small-molecule suppressor of survivin, in patients with advanced, refractory, non-small-cell lung cancer. J Clin Oncol. 2009; 27:4481–4486. [PubMed: 19687333]
11. Wang Q, Chen Z, Diao X, Huang S. Induction of autophagy-dependent apoptosis by the survivin suppressant YM155 in prostate cancer cells. Cancer Lett. 2011; 302:29–36. [PubMed: 21220185]
12. Levine B, Kroemer G. Autophagy in the pathogenesis of disease. Cell. 2008; 132:27–42. [PubMed: 18191218]
13. Giampietri C, Petrungaro S, Padula F, et al. Autophagy modulators sensitize prostate epithelial cancer cell lines to TNFalpha-dependent apoptosis. Apoptosis. 2012; 17:1210–1222. [PubMed: 22923157]
14. Fiorini C, Menegazzi M, Padroni C, et al. Autophagy induced by p53-reactivating molecules protects pancreatic cancer cells from apoptosis. Apoptosis. 2013; 18:337–346. [PubMed: 23238993]
15. Mizushima N, Levine B, Cuervo AM, Klionsky DJ. Autophagy fights disease through cellular self-digestion. Nature. 2008; 451:1069–1075. [PubMed: 18305538]
16. Pattingre S, Tassa A, Qu X, et al. Bcl-2 antiapoptotic proteins inhibit Beclin 1-dependent autophagy. Cell. 2005; 122:927–939. [PubMed: 16179260]
17. Kihara A, Kabeya Y, Ohsumi Y, Yoshimori T. Beclin-phosphatidylinositol 3-kinase complex functions at the trans-Golgi network. EMBO Rep. 2001; 2:330–335. [PubMed: 11306555]
18. Davis IJ, Hsi BL, Arroyo JD, et al. Cloning of an Alpha-TFEB fusion in renal tumors harboring the t(6;11)(p21;q13) chromosome translocation. Proc Natl Acad Sci USA. 2003; 100:6051–6056. [PubMed: 12719541]

NIH-PA Author Manuscript NIH-PA Author Manuscript NIH-PA Author Manuscript

19. Settembre C, Di Malta C, Polito VA, et al. TFEB links autophagy to lysosomal biogenesis. Science. 2011; 332:1429–1433. [PubMed: 21617040]
20. Pena-Llopis S, Vega-Rubin-de-Celis S, Schwartz JC, et al. Regulation of TFEB and V-ATPases by mTORC1. EMBO J. 2011; 30:3242–3258. [PubMed: 21804531]
21. David R. Autophagy: TFEB perfects multitasking. Nat Rev Mol Cell Biol. 2011; 12:404. [PubMed: 21654707]
22. Roczniak-Ferguson A, Petit CS, Froehlich F, et al. The transcription factor TFEB links mTORC1 signaling to transcriptional control of lysosome homeostasis. Sci signal. 2012; 5:ra42. [PubMed: 22692423]
23. Sun ZJ, Chen G, Hu X, et al. Activation of PI3 K/Akt/IKKalpha/NF-kappaB signaling pathway is required for the apoptosisevasion in human salivary adenoid cystic carcinoma: its inhibition by quercetin. Apoptosis. 2010; 15:850–863. [PubMed: 20386985]
24. Sun ZJ, Chen G, Zhang W, et al. Mammalian target of rapamycin pathway promotes tumor-induced angiogenesis in adenoid cystic carcinoma: its suppression by isoliquiritigenin through dual activation of c-Jun NH2-terminal kinase and inhibition of extracellular signal-regulated kinase. J Pharmacol Exp Ther. 2010; 334:500–512. [PubMed: 20484154]
25. Chen G, Hu X, Zhang W, et al. Mammalian target of rapamycin regulates isoliquiritigenin-induced autophagic and apoptotic cell death in adenoid cystic carcinoma cells. Apoptosis. 2012; 17:90–101. [PubMed: 21956714]
26. Sun ZJ, Chen G, Zhang W, et al. Curcumin dually inhibits both mammalian target of rapamycin and nuclear factor-kappaB pathways through a crossed phosphatidylinositol 3-kinase/Akt/IkappaB kinase complex signaling axis in adenoid cystic carcinoma. Mol Pharmacol. 2011; 79:106–118. [PubMed: 20959361]
27. Liu H, Chen G, Zhang W, et al. Overexpression of macrophage migration inhibitory factor in adenoid cystic carcinoma: correlation with enhanced metastatic potential. J Cancer Res Clin Oncol. 2013; 139:287–295. [PubMed: 23064787]
28. Nakahara T, Kita A, Yamanaka K, et al. Broad spectrum and potent antitumor activities of YM155, a novel small-molecule survivin suppressant, in a wide variety of human cancer cell lines and xenograft models. Cancer Sci. 2011; 102:614–621. [PubMed: 21205082]
29. de Bruin EC, Medema JP. Apoptosis and non-apoptotic deaths in cancer development and treatment response. Cancer Treat Rev. 2008; 34:737–749. [PubMed: 18722718]
30. Fimia GM, Piacentini M. Regulation of autophagy in mammals and its interplay with apoptosis. Cell Mol Life Sci. 2010; 67:1581–1588. [PubMed: 20165902]
31. Maiuri MC, Zalckvar E, Kimchi A, Kroemer G. Self-eating and self-killing: crosstalk between autophagy and apoptosis. Nat Rev Mol Cell Biol. 2007; 8:741–752. [PubMed: 17717517]
32. Sharma N, Thomas S, Golden EB, et al. Inhibition of autophagy and induction of breast cancer cell death by mefloquine, an antimalarial agent. Cancer Lett. 2012; 326:143–154. [PubMed: 22863539]
33. Frierson HF Jr, El-Naggar AK, Welsh JB, et al. Large scale molecular analysis identifies genes with altered expression in salivary adenoid cystic carcinoma. Am J Pathol. 2002; 161:1315–1323. [PubMed: 12368205]
34. Niu TK, Cheng Y, Ren X, Yang JM. Interaction of Beclin 1 with survivin regulates sensitivity of human glioma cells to TRAIL-induced apoptosis. FEBS Lett. 2010; 584:3519–3524. [PubMed: 20638385]
35. Roca H, Varsos Z, Pienta KJ. CCL2 protects prostate cancer PC3 cells from autophagic death via phosphatidylinositol 3-kinase/AKT-dependent survivin up-regulation. J Biol Chem. 2008; 283:25057–25073. [PubMed: 18611860]
36. Na YS, Yang SJ, Kim SM, et al. YM155 induces EGFR suppression in pancreatic cancer cells. PLoS One. 2012; 7:e38625. [PubMed: 22723871]
37. Zaytseva YY, Valentino JD, Gulhati P, Evers BM. mTOR inhibitors in cancer therapy. Cancer Lett. 2012; 319:1–7. [PubMed: 22261336]
38. Martina JA, Chen Y, Gucek M, Puertollano R. MTORC1 functions as a transcriptional regulator of autophagy by preventing nuclear transport of TFEB. Autophagy. 2012; 8:903–914. [PubMed: 22576015]

39. Pena-Llopis S, Brugarolas J. TFEB, a novel mTORC1 effector implicated in lysosome biogenesis, endocytosis and autophagy. Cell Cycle. 2011; 10:3987–3988. [PubMed: 22101272]

NIH-PA Author Manuscript

NIH-PA Author Manuscript

NIH-PA Author Manuscript

NIH-PA Author Manuscript
NIH-PA Author Manuscript
NIH-PA Author Manuscript

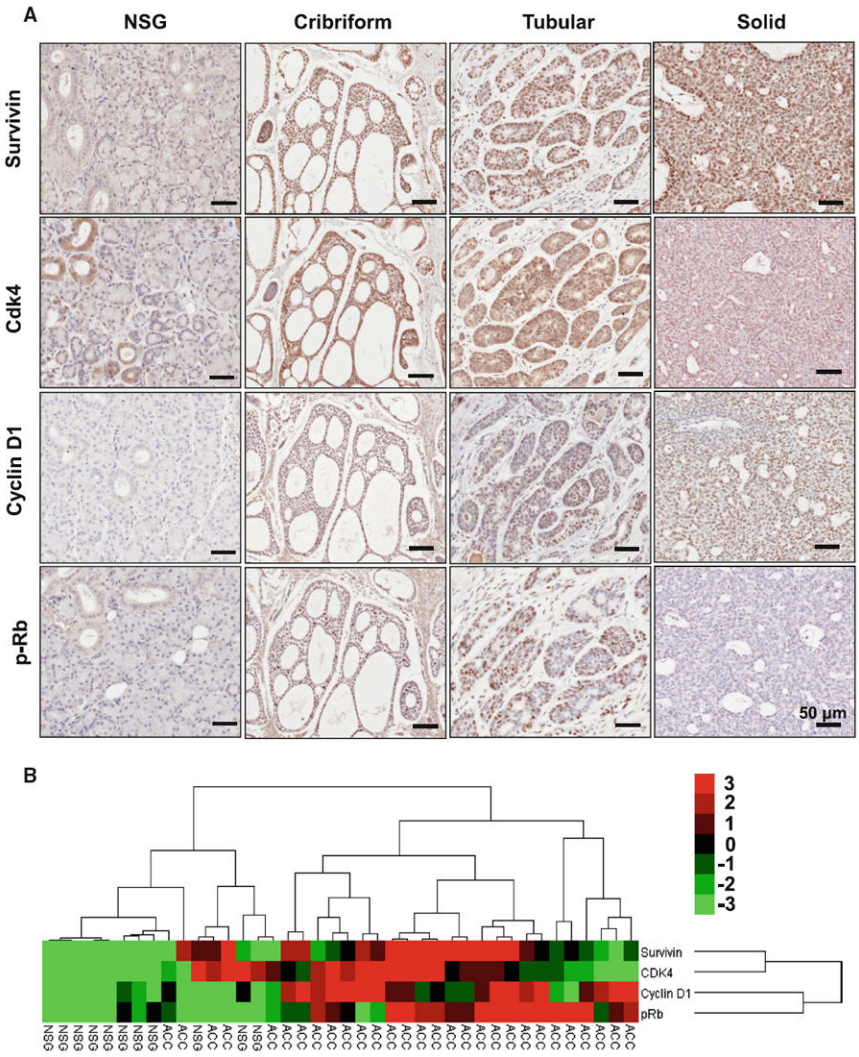

Fig. 1.

Increased expression level of survivin/CDK4/Cyclin D1/p-Rb^{S780} in human salivary gland ACC. **a** Immunohistochemical staining of survivin/CDK4/Cyclin D1/p-Rb^{S780} in cribriform, tubular, and solid ACC as compared with normal salivary gland (NSG). *Scale bar* 50 μm. **b** Clustering analyses of immunohistochemistry of ACC and normal salivary gland (NSG) tissue in which the closeness of the columns directly indicates correlation

NIH-PA Author Manuscript

NIH-PA Author Manuscript

NIH-PA Author Manuscript

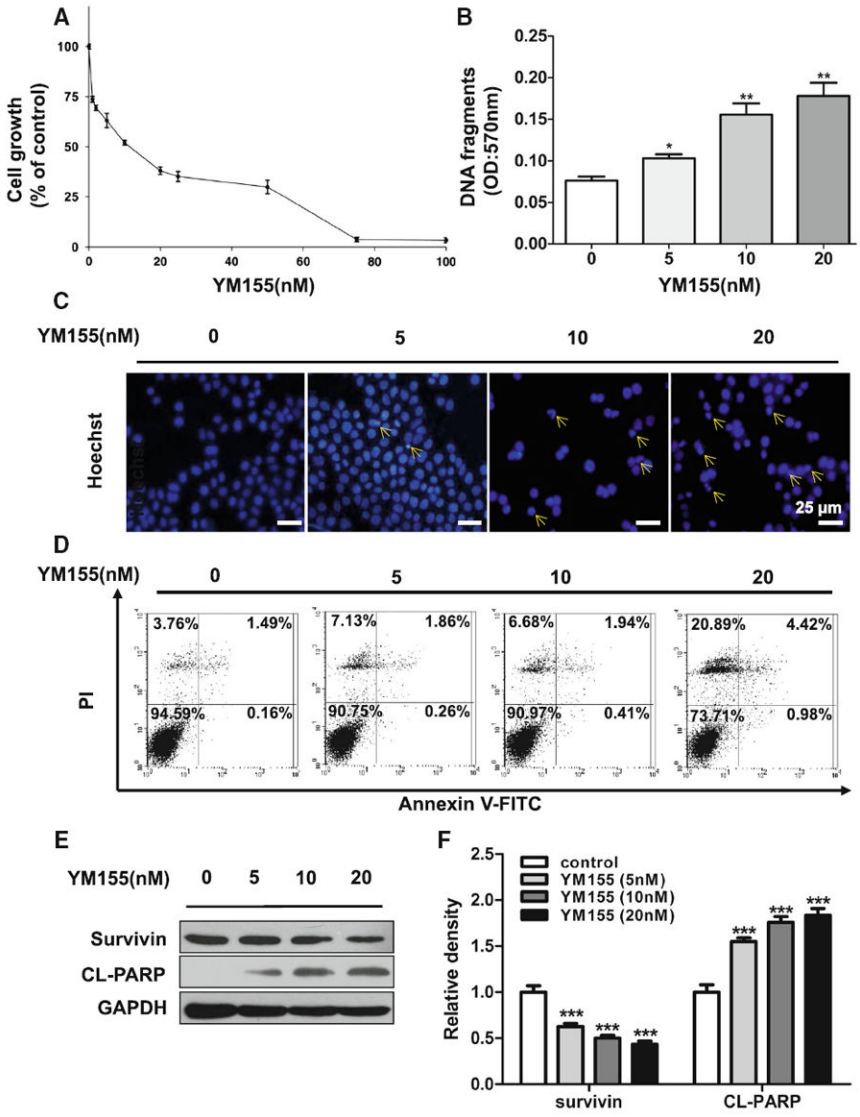

Fig. 2.

YM155 induced cell death in ACC-2 cell line. **a** Cell growth of ACC-2 was measured using an MTT assay after treated with YM155 for 24 h. The viability ratio is normalized by the ratio of the optical density value obtained from the YM155-treated sample divided by that of control group. **b** Cell death detection ELISA analysis of cell apoptosis induced by YM155 in dose-dependent manner in ACC-2 was detected. $*P < 0.05$; $**P < 0.01$ as compared with the control group. One-way ANOVA with post-Dunnett analysis was used. **c** The morphologic changes of ACC-2 treated with YM155 were captured using fluorescence microscopy with Hoechst 33258 staining. *Scale bar* 25 μm. **d** ACC cells were treated with YM155 for 24 h and apoptosis rate was determined by Annexin V-FITC/PI dual labeling using flow cytometry. **e** Cell lysates of the four groups subjected to western blotting with antibodies against survivin and cleaved PARP (CL-PARP), and GAPDH served as a loading control. **f** Relative quantitative data were calculated by ImageJ. $***P < 0.001$ one-way ANOVA with

post-Dunett analysis was used by GraphPad Prism5. The *arrows* indicate chromatin condensation in ACC-2 cells

NIH-PA Author Manuscript
NIH-PA Author Manuscript
NIH-PA Author Manuscript

NIH-PA Author Manuscript
NIH-PA Author Manuscript
NIH-PA Author Manuscript

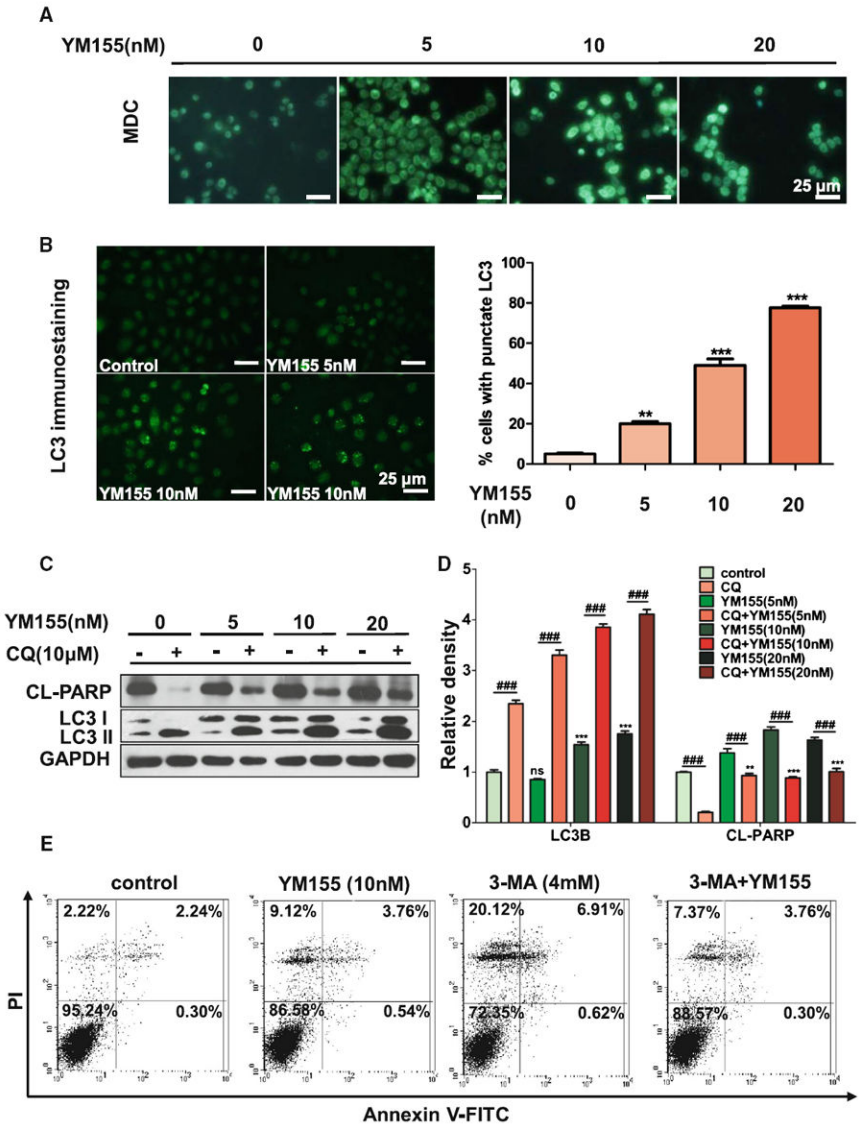

Fig. 3.

YM155 induced autophagy in ACC-2. **a** Representative confocal microscopic images of monodansylcadaverine (MDC) staining. *Scale bar* 25 μm. **b** Representative images of LC3+ cells induced by YM155 treatment by immunofluorescence in left part. *Scale bar* 25 μm. Quantification for punctate pattern of LC3 immunostaining was showed in right part. **c** Increased ratio of LC3II/LC3I and cleaved PARP (CL-PARP) protein level in ACC-2 cells treated with YM155 for 24 h by western blotting. The apoptosis induced by YM155 were attenuated by treated with chloroquine (CQ). **d** Relative quantitative data were calculated by ImageJ. $^{**}P < 0.01$; $^{***}P < 0.001$ one-way ANOVA with post-Dunett analysis was used by GraphPad Prism5. $^{\#\#\#}P < 0.001$ One-way ANOVA with post-Tukey analysis was used by GraphPad Prism5. **e** ACC cells were treated with YM155 or (and) 3-MA for 24 h and apoptosis was determined by Annexin V-FITC/PI dual labeling using flow cytometry

NIH-PA Author Manuscript

NIH-PA Author Manuscript

NIH-PA Author Manuscript

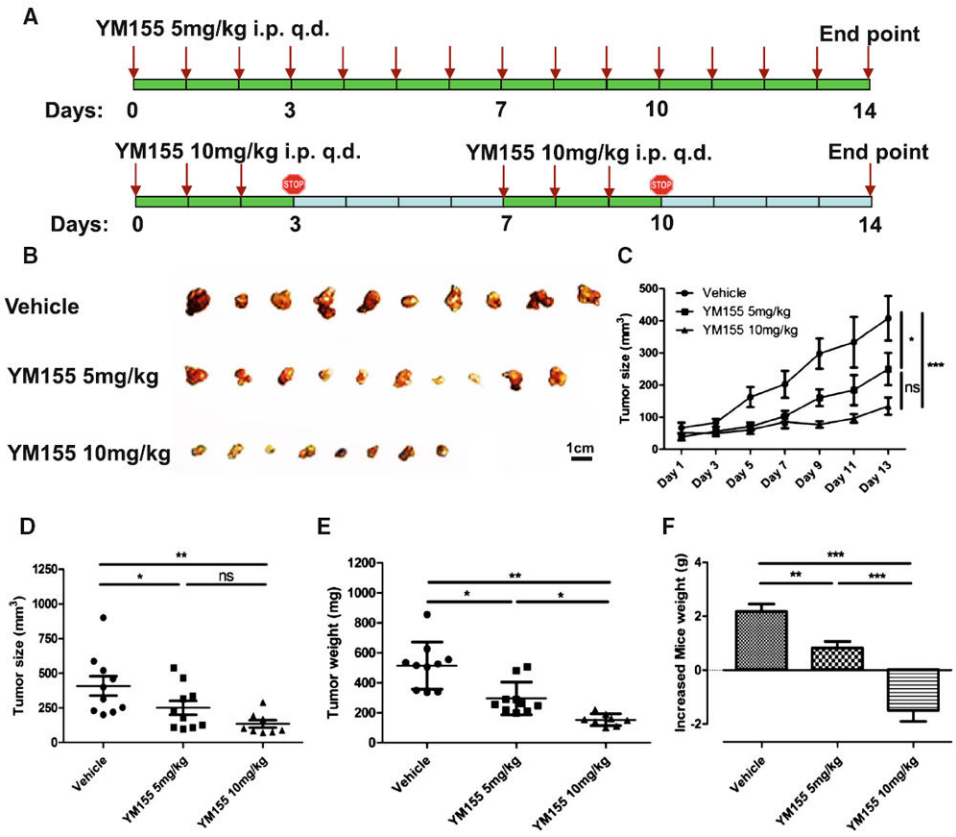

Fig. 4.

YM155 suppressed tumorigenesis in ACC-2 xenograft. **a** A schematic showing a drug delivery strategy for YM155 in the chemotherapeutic tumorigenesis experiment in ACC-2 xenograft in athymic$^{nu/nu}$ mice. Athymic$^{nu/nu}$ mice bearing ACC-2 cells were intraperitoneal injected (i.p.) 100 μL PBS (Vehicle group, $n = 5$), 5 mg/kg YM155 ($n = 5$) for 14 consecutive days or 10 mg/kg YM155 for 3-day continuous infusion per week for 2 weeks. **b** Representative tumor of ACC-2 xenograft. *Scale bar* 1 cm. **c** Tumor size from ACC-2 xenografts in both YM155- and vehicle-treated groups was assessed every other day. *$P <$ 0.05; ***$P < 0.001$ two-way ANOVA with Bonferroni posttest analysis was used by GraphPad Prism5. Quantification of tumor size, **d** and tumor weight, **e** after the animals were sacrificed, **f** body weight of mice was measured daily with normalized to day 1. All values are presented as (mean ± SEM). *$P < 0.05$; **$P < 0.01$; ***$P < 0.001$ one-way ANOVA with post-Tukey analysis was used by GraphPad Prism5

NIH-PA Author Manuscript

NIH-PA Author Manuscript

NIH-PA Author Manuscript

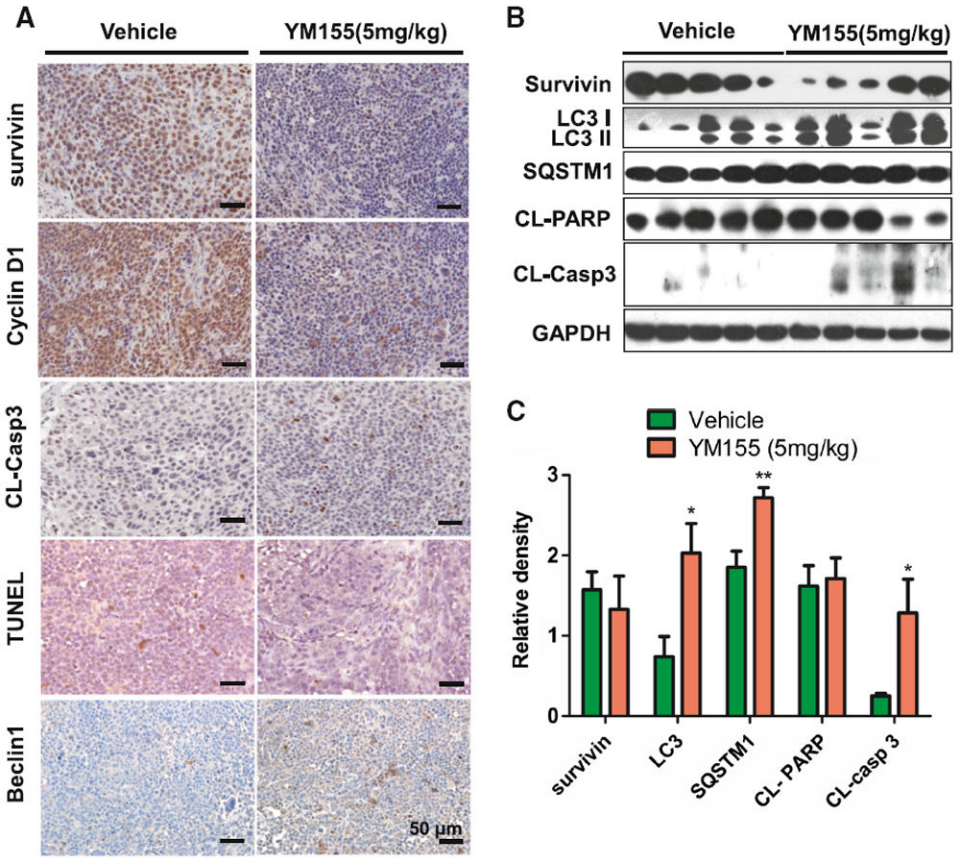

Fig. 5.

YM155 induced cell death and autophagy in ACC xenograft. **a** Immunohistochemical analysis of the survivin, cyclin D1, cleaved caspase 3(CL-Casp3) and Beclin1in both vehicle and YM155-treated ACC-2 xenograft tissues, in situ apoptosis were stained by TUNEL assay. **b** The expression of survivin, LC3II/LC3I, SQSTM1, cleaved PARP (CLPARP) and cleaved caspase 3(CL-Casp3) by western blot. **c** Relative quantitative data were calculated by ImageJ. $*P < 0.05$; $**P < 0.01$ as compared with the control group. Student *t* test was used

NIH-PA Author Manuscript

NIH-PA Author Manuscript

NIH-PA Author Manuscript

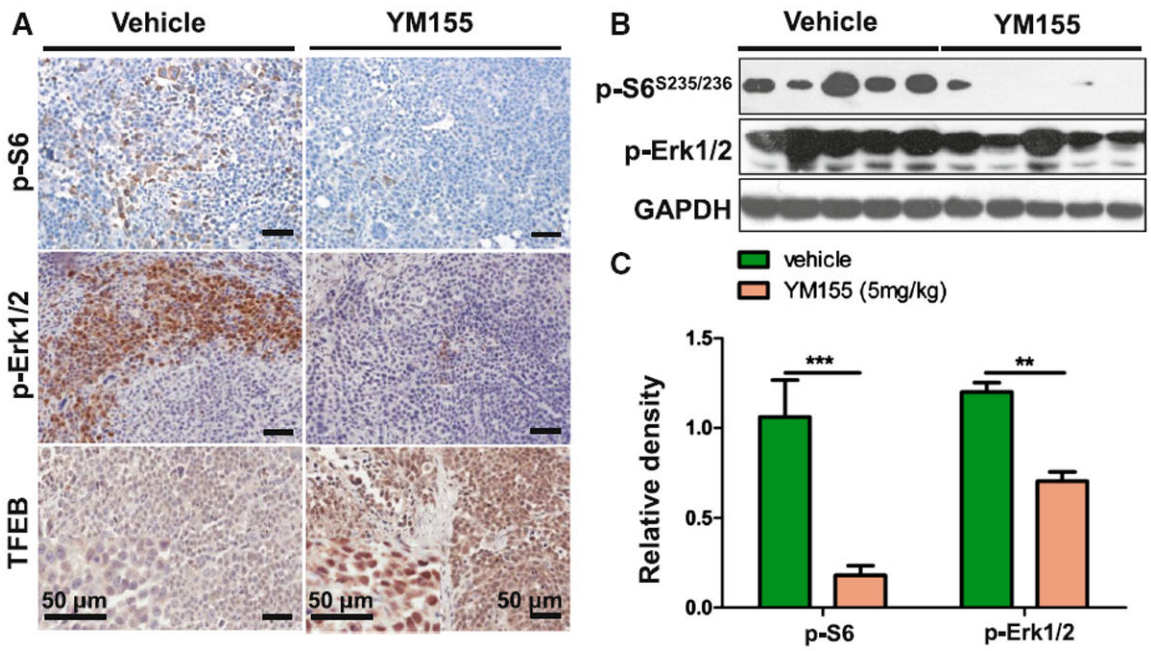

Fig. 6.

YM155 decreased phosphorylation of S6, Erk1/2 and increased nuclear translocation of TFEB. **a** Immunohistochemical analysis of the indicated decrease of p-S6, pErk$^{Thr202/Tyr204}$ and increase nuclear translocation of TFEB in YM155-treated ACC-2 tumor tissues. **b** The expression of p-S6 and pErk$^{Thr202/Tyr204}$ were determined by western blot. **c** Relative quantitative data were calculated by ImageJ. $^{**}P < 0.01$; $^{***}P < 0.001$ as compared with the control group. Student *t* test was used